Physica B 508 (2017) 104–111

Contents lists available at ScienceDirect

Physica B

journal homepage: www.elsevier.com/locate/physb

Study of surface exfoliation on 6H-SiC induced by H_2^+ implantation

L. Zhang[a], B.S. Li[b,*]

[a] Department of Physics, School of Science, Lanzhou University of Technology, Lanzhou 730050, China
[b] Institute of Modern Physics, Chinese Academy of Sciences, Lanzhou 730000, China

ARTICLE INFO

Keywords:
Smart-cut
H_2^+ implantation
Transmission electron microscopy
Exfoliation
Blisters

ABSTRACT

The effect of lattice damage generated by the H_2^+-implantation on exfoliation efficiency in 6H-SiC wafers is investigated. < 0001 > 6H-SiC wafers were implanted with 134 keV H_2^+ ions to ion fluences from 1.5×10^{16} to 5×10^{16} H_2^+ cm^{-2} and subsequently annealed at temperatures from 973 K to 1373 K. The samples were studied by a combination of optical microscopy and transmission electron microscopy. Only after 1373 K annealing for 15 min, blisters and exfoliation occur on the H_2^+-implanted sample surface. With increasing the implantation fluences from 1.5×10^{16} to 3.75×10^{16} H_2^+ cm^{-2}, the exfoliation mean size decreases, while the exfoliation density increases. For the highest fluence of 5×10^{16} H_2^+ cm^{-2}, seldom exfoliations occur on the sample surface. Microstructure analysis shows that exfoliation efficiency is largely controlled by the H_2^+-implantation-induced lattice damage. The depth of the microcrack is related to the implantation fluence. The effect of implantation fluence on dislocation loops, platelet nucleation and growth is investigated.

1. Introduction

Due to its excellent optical and electronic properties, considerable research and development effects have been paid to explore the potential of SiC for optoelectronic application [1,2]. In addition, SiC has a low cross-section for neutron capture and thus presents a low induced activity in neutron irradiation ambient. SiC has excellent chemical, mechanical and structural stabilities, and therefore SiC is regarded as an ideal structural component for working in harsh environment, i.e., as cladding materials for gas-cooled fission reactors [3,4]. SiC has more than 200 polytypes and the hexagonal 4H and 6H ones are regarded as the most promising materials for microelectronic and optoelectronic applications.

Similar abilities have been previously reported for silicon-on-insulator (SOI) structures, SiC-on-insulator (SiCOI) structures also have excellent properties, i.e., low power dissipation and high resistance to radiation [5]. SiCOI structures have been achieved by the Smart-cut technology. There are three main steps in the smart-cut technology: (i) hydrogen ion implantation, (ii) wafer bonding, and (iii) fracture to achieve thin layer transfer [6,7]. To investigate the mechanism of ion-cut process, it is necessary to research the defect formation and recovery process in H-implanted SiC. Jiang et al. [8] investigated the implantation-induced defect annealing with temperature in H_2^+-implanted 6H-SiC via Rutherford backscattering in channeling geometry. The gradual recovery over a wide temperature range and no complete recovery even at 1070 K for 2.25×10^{16} H_2^+ cm^{-2} and below at 300 K implantation were observed. At intermediate fluences between 2.25×10^{16} H_2^+ cm^{-2} and 7.5×10^{16} H_2^+ cm^{-2}, the recovery processes were relatively rapid up to 870 K annealing due to higher defect concentration formed. At high fluences of 7.5×10^{16} H_2^+ cm^{-2} and above, no significant recovery processes were observed upon 870 K annealing due to amorphous structure formed during H_2^+-implantation. Gregory et al. [9] discussed the relationship of implantation temperature and threshold fluence for exfoliation in H^+-implanted 4H-SiC. The threshold fluence decreased with increasing implantation temperature. It is attributed to the increase in platelet nucleation with elevated implantation temperature [10]. Grisolia et al. [11] reported the growth process of H-implantation induced platelets in 6H-SiC. The activation energy for platelet growth is approximately 3.4 eV. As for the ion-cut process in H^+-implanted Si, the implantation-induced defects can affect the microcrack nucleation and growth. There are extensive studies on implantation-induced defects and recovery processes in H^+-implanted Si [10,12,13]. However, until now less attention has been paid to the dependence of the exfoliation on H-implantation induced lattice disorder and thermal annealing in SiC [9,14]. Understanding the nature and formation of the defect clusters in H-implanted-SiC will contribute to the interpretation of ion-cut mechanism of SiC.

In the present work, we report a study of the dependence of exfoliation efficiency on H-implantation induced lattice disorder.

* Correspondence to: Laboratory of Advanced Nuclear Materials, Institute of Modern Physics, CAS, Lanzhou 730000, China.
E-mail address: b.s.li@impcas.ac.cn (B.S. Li).

http://dx.doi.org/10.1016/j.physb.2016.12.027
Received 18 October 2016; Received in revised form 20 December 2016; Accepted 21 December 2016
Available online 23 December 2016

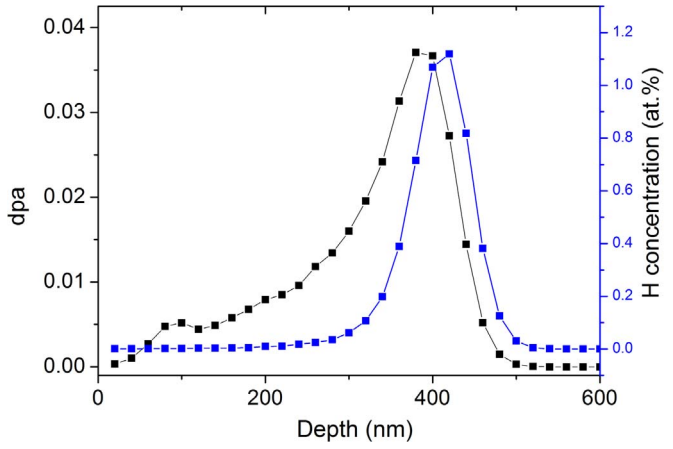

Fig. 1. Depth profiles of the damage level and H concentration in 6H-SiC implanted with 134 keV H_2^+ ions to a fluence of 0.5×10^{15} cm^{-2}.

2. Experimental procedures

The < 0001 > -oriented 6H-SiC single-crystal wafers were obtained from MIT company with a dimension of $10\times10\times0.35$ mm^3. Hydrogen implantation experiments were performed at the 320 kV high-voltage platform equipped with an ECR (Electron Cyclotron Resonance) ion source in Institute of Modern Physics, Chinese Academy of Sciences. Hydrogen molecular beams (H_2^+) with an energy of 134 keV were chosen to implant samples close to the surface normal direction at room temperature (RT). The beams were magnetically scanned against a stationary ion beam to provide uniform ion fluence across the sample. To investigate the influence of implantation-induced damage and H concentration on the process of ion-cut, four different implantation fluences, which are 1.5×10^{16} H_2^+ cm^{-2}, 2.5×10^{16} H_2^+ cm^{-2}, 3.75×10^{16} H_2^+ cm^{-2} and 5×10^{16} H_2^+ cm^{-2}, were chosen. The implantation damage in displacements per atom (dpa) and concentration were simulated by SRIM-2013 , as shown in Fig. 1. The mean projected range R_p is approximately 393 nm with a straggling ΔR_p of approximately 46 nm. What's more, these implantation fluences correspond to the maximum damage and a peak H concentration of 0.11 dpa and 3.3 at%, 0.19 dpa and 5.5 at%, 0.26 dpa and 7.7 at%, 0.37 dpa and 11 at%, respectively [15]. Post-implantation, the samples were cut into four pieces upon isochronal annealing for 15 min under argon gas flow over the temperature range from 973 K to 1373 K. After annealing, the sample was quickly cooled to RT under argon gas flow.

The evolution of the surface morphology properties of the implanted as well as un-implanted samples was analyzed by Olympus optical microscopy. The magnification was 1000 times, which is able to observe micro-scale bubbles and exfoliation on the sample surface. The microstructural evolution as a function of the implantation fluence was investigated with Tecnai G20 transmission electron microscopy (TEM) equipped with a double tilt goniometer stage. Cross-sectional TEM (XTEM) images were taken at 200 kV. The fabrication process of XTEM samples were described in our recent paper [16]. The bubbles and cracks were imaged in under-focused and over-focused conditions to highlight the bubble and crack edges with Fresnel contrast. The observed images of H implantation-induced stacking faults and dislocation loops were taken from cross sections of 6H-SiC along a $[01\bar{1}0]$ zone axis. The stacking faults and dislocation loops observed in the damage band were identified on cross sectional high resolution images taken along a $[11\bar{2}0]$. The damage band was examined in conventional bright-field (BF) mode and weak-beam dark-field (WBDF) mode with the image condition: (g, 3g/5g), g=0002 and g=$\bar{2}$ 110 near $z=01\bar{1}0$, where g is the diffraction vector and z is the zone axis. *S* in the TEM image denotes the implanted surface of the sample.

3. Results and discussion

A series of surface morphology images of the annealed and as-implanted sample obtained by optical microscopy. Before and after annealing at 973 K or 1173 K, whatever the implantation fluence performed, the sample surfaces have not any change as compared to the un-implanted sample (not shown). However, after 1373 K annealing for the implanted samples, many bright contrasts appear as circular in shape on the surface, as shown in Fig. 2. The observed contrasts are attributed to blisters. In addition, some blisters broke through the sample surface to form exfoliation. The observed blisters and exfoliation are correlated with the implantation fluence. Fig. 2 shows that the mean sizes of blisters and exfoliation decrease with increasing fluence.

In order to evaluate the exfoliation behavior as a function of the implantation fluence, three parameters were introduced to quantify the exfoliation: the exfoliation efficiency A_{ex}; the mean exfoliation area S_{ex}; the exfoliation density D_{ex} [17]. The exfoliation efficiency is defined as $A_{ex}\%=A_{ex}^{total}/A_{sample}^{total}.100$, where A_{ex}^{total} is the total exfoliated area obtained by the sum of the individual exfoliated areas and A_{sample}^{total} is the total area of the image. The mean exfoliation area S_{ex} is determined by $S_{ex}=A_{ex}^{total}/N_{ex}$, where N_{ex} is the total number of individual exfoliations measured in the image. The exfoliation density D_{ex} is determined by $D_{ex}=N_{ex}/A_{sample}^{total}$.

These parameters were evaluated from optical microscopy images and the results were given in Table 1. With increasing implantation fluence, the exfoliation efficiency A_{ex} and the exfoliation mean size S_{ex} decrease, while the exfoliation density D_{ex} initially increases and reaches a maximum value of 3.5×10^{-3} and finally decreases.

The exfoliation efficiency A_{ex}, the exfoliation mean size S_{ex}, and the exfoliation density D_{ex} are correlated to exfoliation efficient cavities in the H-implantation-induced damaged region. According to the present experimental results, the nucleation of exfoliation efficient cavities is correlated to the concentration of gas atoms. In general, the increase in concentration of gas atoms can enhance the nucleation of exfoliation efficient cavities. The following exfoliation mechanisms can explain the present experimental results. After 1.5×10^{16} H_2^+ cm^{-2} implantation, the internal pressure of the exfoliation efficient cavities is not high enough to overcome the fracture stress of silicon carbide. A cleavage assisted coalescence process occurs between neighbor exfoliation efficient cavities due to the high stress introduced in the area between neighboring exfoliation efficient cavities. Exfoliation efficient cavities coalescence occurs upon annealing. Feng et al. [18] gave an internal pressure model that the internal pressure explodes blister caps. The pressure is inversely proportional to r^2, where r is the radius of a blister. The increase in size of exfoliation efficient cavities induces the internal pressure of exfoliation efficient cavities which finally meets the threshold pressure for exploding blister caps. Hence, the A_{ex} value and S_{ex} value are maximum at a fluence of 1.5×10^{16} H_2^+ cm^{-2}, which is smaller than the threshold dose for exfoliation in H^+-implanted 4H-SiC at RT as reported by Gregory et al. [9]. The authors reported that the threshold dose for exfoliation is 4.5×10^{16} H^+ cm^{-2} in H^+-implanted 4H-SiC at RT and followed by 1223 K annealing for 15 min. Two possible reasons can explain why the present dose is smaller than that reported by Gregory et al. [9]. One reason is that our annealing temperature is 1373 K which is higher than 1223 K mentioned by Gregory et al. [9]. The increase in annealing temperature will elevate the diffusion ratio of H_2 molecules in the SiC, and therefore migration and agglomeration into platelets of dense H_2 molecules lead to the preferential occurrence of exfoliation. Another reason is that molecular H_2 implantation in the present study would be different from atomic H implantation. Considering the chemical properties that the implanted atomic H is more preferential to react with Si and C atoms as compared to the implanted molecular H_2, and therefore the decrease of H_2 molecules accumulates into platelets. In the case of exfoliation of H^+-implanted Si, the increase in the intensity of the elastic out-of-plane tensile strain facilitates the growth of platelets. In the previous report